



Regeneration energy analysis on desiccant wheel system in curling arena for the Winter Olympics



Bowen Guan ^a, Xiaohua Liu ^b, Xinkle Wang ^a, Tao Zhang ^{b,*}, Ziqi Zhou ^c

^a School of Human Settlements and Civil Engineering, Xi'an Jiaotong University, Xi'an, Shaanxi, 710054, China

^b Department of Building Science, Tsinghua University, Beijing, 100084, China

^c China Construction First Group Corporation Limited, Beijing, 100161, China

ARTICLE INFO

Keywords:
Desiccant wheel
Regeneration
Energy conservation
Carbon emission
Curling arena

ABSTRACT

Excess moisture is an important problem for the curling arena, since the moisture can condense onto the ice surface, destroying the smoothness and flatness of the ice surface. So far, air dehumidification and desiccant regeneration issues in ice rinks, such as curling arenas, are relative unknown and poorly reported in previous studies. Thus, on-site test and numerical simulation were carried out in this study to investigate the regeneration energy performance of a desiccant wheel system applied in the Winter Olympic curling arena. Results reveal that using the low-temperature and low-humidity outdoor air as the regeneration air (Strategy I) will perform better than using the high-temperature and high-humidity indoor air as the regeneration air (Strategy II) during the 2022 Winter Olympics. In the basic case, the coefficient of regeneration performance of the system can be improved by 41.2% and the carbon emission for the regeneration process can be reduced by 42.0% by Strategy I, compared to Strategy II. During the entire Winter Olympic month, the carbon emission for desiccant regeneration can be reduced by 19.4% by Strategy I. Moreover, a quick and approximate method without iterative processes is developed for regeneration air selection in similar ice arenas.

1. Introduction

Smoothness and flatness of the ice surface are essential requirements for the ice rink arena, particularly for the curling arena. According to regulations of the World Curling Federation, the dew point temperature of the air near the ice surface is required to be controlled below -4°C , indicating a required air humidity ratio below 2.8 g/kg. Excess moisture is an important problem for the arena, since the moisture can condense onto the ice surface, destroying the smoothness and flatness of the ice surface. To strictly avoid excess moisture, it is inevitable to introduce the air-dehumidification system into the arena. Different from residential buildings and office buildings requiring dehumidified air supply in summer while humidified air supply in winter, the curling venue nearly always requires dehumidified air supply even in winter.

Desiccant wheel system is a feasible system to achieve the above-mentioned process to dehumidify the dew point temperature of the feed air below -4°C [1–3]. Desiccant regeneration is essential for continuous operation of the air-dehumidification system. Both indoor air and outdoor air can be utilized as the regeneration air for desiccant regeneration [4–6]. The regeneration air selection plays an important role in

determining the required regeneration temperature and deciding whether the low-grade energy can be used for regeneration for energy conservation [7,8]. To minimize regeneration energy consumption, high-temperature and low-humidity air is desired and expected to be used as the regeneration air [9,10].

With respect to using outdoor air as the regeneration air, Caliskan et al. [11] proposed a desiccant wheel system, and the results revealed that the system shows good energy performance by the virtue of combining a sensible heat wheel and an evaporative air cooler with the desiccant wheel. Rjibi et al. [12] investigated a desiccant wheel system powered by air solar collectors coupled to an insulated greenhouse, wherein the outdoor air is used as the regeneration air for desiccant regeneration. The results revealed that the utilization of the proposed desiccant wheel system allows saving 9396 kWh/year of electric energy in comparison to the conventional system. Ren et al. [13] integrated the photovoltaic thermal collector and thermal energy storage unit using phase change materials with a desiccant wheel system, and tested the system performance when using outdoor air as the regeneration air. The results demonstrated that the solar thermal contribution index increases from 82.6% to 100.0% when the regeneration temperature reduces from 70 to 60°C . It is indicated that the photovoltaic thermal collector-solar

* Corresponding author.

E-mail address: zt2015@mail.tsinghua.edu.cn (T. Zhang).

Nomenclature	
COP_{reg}	coefficient of regeneration performance
CEI_{reg}	carbon emission intensity for regeneration (kg/h, kg)
$c_{p,a}$	specific heat capacity of air (kJ/(kg·°C))
$c_{p,d}$	specific heat capacity of desiccant (kJ/(kg·°C))
$c_{p,w}$	specific heat capacity of water (kJ/(kg·°C))
d	hydraulic diameter of desiccant channel (m)
D_A	diffusion coefficient for water vapor
D_S	surface diffusion coefficient for water in absorption state
f	ratio of solid area to channel area
H	height (m)
h	specific enthalpy (kJ/kg)
k	convective heat transfer coefficient (W/(m ² ·°C))
k_m	convective mass transfer coefficient (kg/m ² ·s)
m	flow rate (kg/s)
P	power consumption (kW)
Q	heating capacity (kW)
q_g	lower calorific value of nature gas (kJ/m ³)
RH	relative humidity (%)
RS	rotation speed (r/h)
r	latent heat of vapor vaporization of moisture (kJ/kg)
r_s	adsorption heat (kJ/kg)
u_a	air velocity (m/s)
V_g	nature gas consumption in volume (m ³)
W	water content of the absorbent (kg/kg)
<i>Greek symbols</i>	
α	conversion factor (m ³ -gas/kWh-electricity)
γ_v	volume ratio of the adsorbent in the wheel
Δt	temperature difference (°C)
$\Delta \omega$	humidity ratio difference (g/kg)
δ_H	energy unbalance rate (%)
δ_m	mass unbalance rate (%)
ε	porosity
η	heat exchanger effectiveness
λ_d	heat conductivity of absorbent (W/(m ² ·°C))
ρ_a	air density (kg/m ³)
ρ_{ad}	absorbent density (kg/m ³)
ρ_d	equivalent desiccant density taking the water content into consideration (kg/m ³)
ξ_e	carbon emission factor of electricity (kg-CO ₂ /kWh-electricity)
ξ_g	carbon emission factor of nature gas (kg-CO ₂ /m ³ -gas)
τ	time (s)
ω	humidity ratio (g/kg)
<i>Subscripts</i>	
a	feed air
d	desiccant
h,I	Heater I
h,II	Heater II
in	inlet
latent	latent heat
math	mathematical model
out	outlet
r	regeneration air
sim	simplified method

air heater and air-based thermal energy storage unit can be potentially used to regenerate desiccant wheels. Liu et al. [14] developed a two-stage desiccant wheel system using outdoor air as the regeneration air for low latitude isolated islands. The desiccant wheel is regenerated via photovoltaic power generation device and solar thermal collector. It is indicated that the system dehumidification capacity increases by 0.9–2.7 g/kg for every 10 °C regeneration temperature increasing. Chen et al. [15] studied a desiccant evaporative combined chilled air/chilled water system, wherein the desiccant is regenerated by outdoor air. A regeneration temperature above 60 °C is recommended in moderate humidity regions, while a regeneration temperature above 70 °C is recommended in high humidity regions. El Loubani et al. [16] investigated a desiccant wheel system regenerated via an auxiliary heater and a Trombe wall, and revealed that 55% energy can be saved by using the Trombe wall in comparison to only relying on the auxiliary heater. Zhou [17] analyzed performance of a solar-assisted desiccant wheel system, and it is demonstrated that energy efficiency of the system is at least 50% greater than that of a conventional system, in terms of the power consumption. Comino et al. [18] presented a study of a desiccant wheel system, and demonstrated that the minimum supply air temperatures the maximum feed air dehumidification are obtained in the circular sector closest to the regeneration side. Dadi and Jain [19] conducted research on a desiccant wheel system applied in hot and humid weather of India, and the results indicated that the system performs better under in hot and humid climatic conditions because of the significant humidity ratio reduction of feed air.

With respect to using indoor air as the regeneration air, Ukai et al. [20] numerically analyzed performance of a desiccant wheel system regenerated by indoor air in hot and humid climate, and the results showed that energy performance of the system depends not only on the inlet air condition to desiccant wheel but also on designed supply air humidity. Fong and Lee [21] derived new perspectives in desiccant wheel system when using indoor air as the regeneration air. It is found

that the system can provide tangible cooling capacity both with and without the regeneration heat, and the wheel should be operated at a high rotation speed together with a sensible heat exchanger in the absence of regeneration heat, while the wheel should be operated at a low speed with a sensible heat exchanger and a regenerative air evaporative cooler in the presence of regeneration heat. Kabeel and Abdelgaiad [22] numerically investigated effects of solar energy and phase change material on the energy saving of desiccant wheel system using indoor air as the regeneration air, and it is demonstrated that the electrical energy consumption can be saved by 60.9%–90.0% by integrating the solar air collector and thermal storage unit with the desiccant wheel system. Shahzad et al. [5] carried out tests on a desiccant wheel system coupled with a heat recovery wheel and an M-Cycle indirect evaporative cooler. It is demonstrated that its coefficient of thermal performance is 60–65% higher than the other system when providing same supply air conditions. Saputra et al. [23] discussed the effect of the regeneration heat input on the dehumidification performance of a desiccant wheel system regenerated by indoor air. It is shown that operation with appropriate control of the regeneration air flow rate as well as the optimal wheel rotation speed contribute to inhibiting the system's dehumidification performance decline. Habib et al. [24] carried out seasonal transient simulations of an integrated desiccant wheel system using return air as the regeneration air, and a solar fraction of 56.2% and a coefficient of thermal performance of 1.52 could be achieved by the system. Heidarnejad et al. [25] investigated a solar desiccant cooling system coupled with a ground source heat exchanger. It is shown that the system coefficient of performance and daily average solar fraction significantly decrease with the desiccant wheel performance reduction. Tian et al. [26] presented investigation on a coupled heat pump desiccant wheel system applied in the nearly zero energy building in Shanghai, wherein return air is used for desiccant regeneration. It is demonstrated that the system shows a performance improvement in both indoor environment control and energy conservation in

comparison to the conventional air conditioner. Asadi and Roshanzadeh [27] improved performance of a two-stage desiccant cooling system by analyzing different regeneration configurations, wherein the regeneration air steam contains 50% outdoor air and 50% indoor air. It is found that, for each system configuration, there is an optimum combination of regeneration temperatures for achieving the maximum thermal coefficient of performance and exergy efficiency.

Although considerable efforts have been made to propose energy-efficient design for desiccant wheel systems applied in different types of buildings, so far, the related issues in ice rinks, such as curling arenas, are relative unknown and poorly reported in previous studies. Thus, on-site measurements were implemented in this study to reveal performance of the desiccant wheel system applied in the Winter Olympic curling venue. Moreover, regeneration performances of the system using outdoor air and using indoor air as the regeneration air during the Winter Olympics were respectively predicted and compared by numerical simulation. Contributions of this study can be summarized as follows: (i) this study provides recommendations for using indoor air or outdoor air as the regeneration air during the 2022 Beijing Winter Olympic Games; (ii) a quick and approximate regeneration air selection method without complex iterative processes is presented to provide reference for optimizing desiccant wheel systems in similar ice arenas.

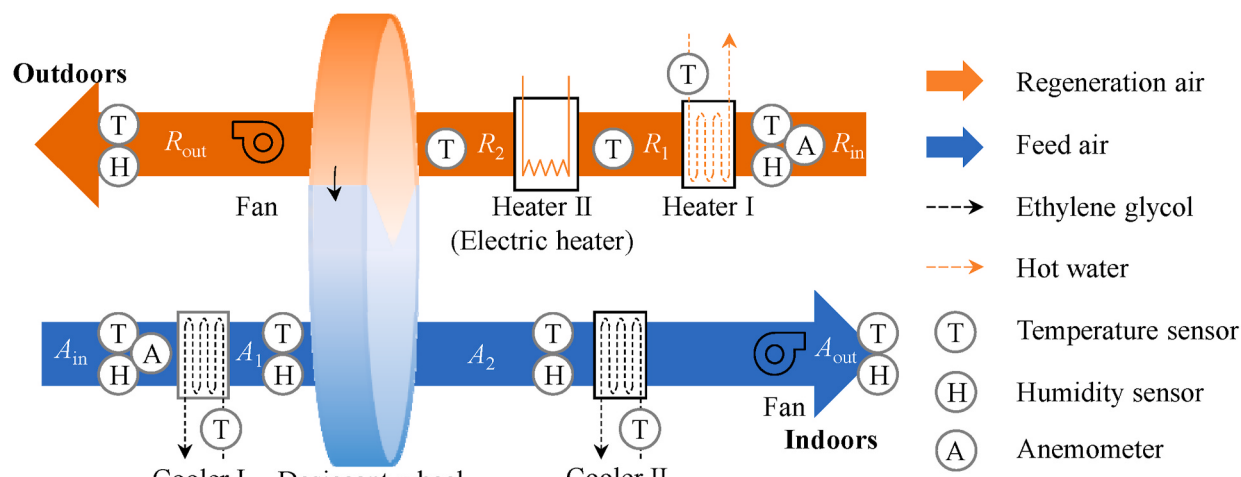
2. Methodology

2.1. System description

Applied in the National Aquatics center of Beijing, China, four desiccant wheel systems provide dry air to the curling venue for avoiding excess moisture. As the four systems are same with each other, one of them is selected as the objective system in this study. The system configuration is shown in Fig. 1 (a). The desiccant wheel is the core device undertaking the latent load in the system. The honeycombed desiccant wheel is fabricated with silica gel. Furthermore, the wheel diameter and thickness are 1.3 m and 0.4 m, respectively, and its dehumidification/regeneration section area ratio is 3:1, with a rotation speed of 10 r/h during the test period.

There are two heaters and two coolers operating in the system for adjusting air temperature. Cooler I and Cooler II are cooling coils with ethylene glycol flowing inside the tube to provide cooling to process air. The cooled ethylene glycol is prepared by chillers in the central cooling plant. Moreover, Heater I is a heating coil with hot water flowing inside the tube to provide heating to the regeneration air. The hot water at an inlet temperature of around 45 °C is from the municipal heat supply network. In addition, Heater II is an electric heater to precisely regulate the air temperature at R_2 (regeneration temperature) corresponding to the required supply air humidity. The electric power consumed by Heater II comes from the electric grid.

There are two air steams flowing through the system, i.e., the feed air steam and the regeneration air steam. With respect to the feed air steam,



(b)

(a)



(c)

Fig. 1. schematic diagram of the desiccant wheel system: (a) system configuration, (b) photograph of the system, and (c) competition venue.

the air (A_{in}) is pre-cooled by Cooler I, and then it is dehumidified by the desiccant wheel. As the dehumidification process is also a heating process, the air after dehumidification (A_2) is further cooled by Cooler II, and then it is supplied into indoors. With respect to the regeneration air steam, air at the state of R_{in} is successively heated by Heater I and Heater II to reach the regeneration temperature. And then the regeneration air at R_2 flows through the desiccant for moisture absorption. The air after desiccant regeneration (R_{out}) is exhausted to outdoors.

2.2. On-site measurements

To prepare for predicting the system performance during the 2022 Winter Olympics, on-site measurements were carried out on October 23, 2021, on which day a test event was held. To investigate the system's dehumidification performance and regeneration energy consumption, feed air and regeneration air parameters at different locations were monitored during the test period. The locations of measuring points are depicted in Fig. 1 (a). The air flow rate is obtained based on the air duct size and the measured air velocity distribution of the duct section. As the fans operated at a fixed frequency, the feed air and regeneration air flow rates could be regarded as constants during the test period. Moreover, inlet temperatures of the hot water and ethylene glycol were monitored by temperature sensors. In addition, power consumption of Heater II was monitored by the existing power meter. The precision characteristics of the mentioned measuring instruments are listed in Table 1.

2.3. Mathematical model and validation

This study aims to predict and optimize performance of the desiccant wheel system during the 2022 Beijing Winter Olympics. A mathematical model in the previous study [28] is adopted to predict the system performance under variable weather conditions. The software Matlab 2019b is used to perform the simulation. Main equations of the adopted model are listed in Table 2. The equations can be solved with the finite difference method, and feed air and regeneration air parameters at exits of the desiccant wheel can be obtained.

To prove the desiccant wheel model feasible to predict performance of the objective system, numerical results by the model are compared with on-site test results during the test event. Air parameter differences between the inlet and outlet of the wheel are introduced to evaluate the model accuracy, expressed as Eqs. (5) and (6), respectively:

$$\Delta t_a = t_{a,2} - t_{a,1} \quad (5)$$

$$\Delta \omega_a = \omega_{a,2} - \omega_{a,1} \quad (6)$$

where $t_{a,1}$ and $t_{a,2}$ denote feed air temperatures at A_1 and A_2 (Fig. 1 (a)), respectively, and $\omega_{a,1}$ and $\omega_{a,2}$ denote feed air humidity ratios at A_1 and A_2 , respectively.

On-site measurements were carried out from 8:00 to 18:00 on the day when the test event was held. The competition phase indicates the time period when the competition is going on, while the commissioning phase indicates the remaining time period. Comparison results are

Table 1
Specifications of measuring devices.

Parameter	Device	Accuracy	Range
Air	Temperature	Thermocouple	$\pm 1.5\%$ $0\text{--}400^\circ\text{C}$
	Humidity	Capacitive humidity sensor	$\pm 2\%$ RH $0\text{--}100\%$ RH
	Velocity	Thermal anemometer ball	± 0.03 m/s $0\text{--}20$ m/s + 5%
Hot water	Temperature	Thermocouple	$\pm 0.1^\circ\text{C}$ $-50\text{--}100^\circ\text{C}$
Ethylene glycol	Temperature	Thermocouple	$\pm 0.1^\circ\text{C}$ $-50\text{--}100^\circ\text{C}$
Electricity	Power	Three-phase power meter	$\pm 0.2\%$ –

Table 2
Mathematical model for desiccant wheel.

Expression	
Energy conservation of air	$\frac{1}{u_a} \frac{\partial t_a}{\partial \tau} + \frac{\partial t_a}{\partial z} = \frac{4k}{\rho_a c_{p,a} u_a d} (t_d - t_a)$ (1)
Mass conservation of air	$\frac{1}{u_a} \frac{\partial \omega_a}{\partial \tau} + \frac{\partial \omega_a}{\partial z} = \frac{4k_m}{\rho_a u_a d} (\omega_d - \omega_a)$ (2)
Energy conservation of the wheel	$\rho_d \left(c_{p,d} + \frac{\rho_{ad} \gamma_v}{\rho_d} c_{p,w} W \right) \frac{\partial t_d}{\partial \tau} + \gamma_v \rho_{ad} c_{p,w} t_d \frac{\partial W}{\partial \tau} = \lambda_d \frac{\partial^2 t_d}{\partial z^2} + r_s \rho_{ad} \gamma_v \frac{\partial W}{\partial \tau} + \frac{4k}{df} (t_a - t_d)$ (3)
Mass conservation of the wheel	$\varepsilon \rho_a \frac{\partial \omega_d}{\partial \tau} + \rho_{ad} \frac{\partial W}{\partial \tau} = \rho_a \varepsilon D_A \frac{\partial^2 \omega_d}{\partial z^2} + \rho_{ad} D_S \frac{\partial^2 W}{\partial z^2} + \frac{4k_m}{\gamma_v df} (\omega_a - \omega_d)$ (4)

z : wheel thickness direction; θ : wheel angular direction.

shown in Fig. 2. Root Mean Square Error (RMSE) is introduced to evaluate the discrepancy between the numerical results and the test results, as expressed in Eq. (7):

$$RMSE = \sqrt{\frac{1}{N} \sum_{i=1}^N (y_i - y_{\text{num},i})^2} \quad (7)$$

where N is the sample size, y_i is the test result, and $y_{\text{num},i}$ is the numerical result.

As shown in Fig. 2, RMSEs for Δt_a and $\Delta \omega_a$ are 0.6°C and 0.3 g/kg , respectively. Discrepancies between the numerical results and test results are less than 15% for both Δt and $\Delta \omega$, and thus, the model accuracy is validated.

In addition, for Cooler I, Cooler II, and Heater I, the heat exchanger effectiveness (η) is used to calculate the air temperature at the exit of the heat exchangers ($t_{a,\text{ex}}$), as expressed in Eq. (8).

$$(t_{a,\text{en}} - t_{a,\text{ex}}) = (t_{a,\text{en}} - t_{l,\text{en}}) \cdot \eta \quad (8)$$

where $t_{a,\text{en}}$ is the air temperature at the entrance of the heat exchanger, and $t_{l,\text{en}}$ is the inlet hot water temperature for Heater I while the inlet ethylene glycol temperature for Coolers I and II. Moreover, as Heater II is an electric heater and $t_{a,\text{ex}}$ of Heater II is regulated by the electric heater for achieving a precise supply air humidity control, its power consumption in numerical simulation is determined by the required regeneration temperature corresponding to the required supply air humidity.

2.4. Evaluation indices

2.4.1. Coefficient of regeneration performance

In order to assess the regeneration energy consumption performance when the desiccant wheel system accomplishing a given dehumidification process, the coefficient of regeneration performance (COP_{reg}) is introduced as Eq. (9):

$$COP_{\text{reg}} = \frac{Q_{\text{latent}}}{P_{h,I} + P_{h,II}} = \frac{m_a r (\omega_{a,1} - \omega_{a,2})}{P_{h,I} + P_{h,II}} = \frac{m_r r (\omega_{r,out} - \omega_{r,2})}{P_{h,I} + P_{h,II}} \quad (9)$$

where Q_{latent} is the latent heat, m_a and m_r are the feed air and regeneration air flow rates, respectively, r is the latent heat of vaporization of moisture, $\omega_{r,out}$ and $\omega_{r,2}$ are regeneration air humidity ratios at R_{out} and R_2 (Fig. 1(a)), respectively, $P_{h,I}$ is the equivalent power consumption of Heater I, and $P_{h,II}$ is the electricity consumption of Heater II (electric heater). As the heating of Heater I is provided by hot water from the municipal heat supply network, $P_{h,I}$ has to be calculated according to Eq. (10) [29].

$$P_{h,I} = \frac{V_g}{\alpha} = \frac{Q_{h,I}}{q_g \cdot \alpha} = \frac{m_r (h_{r,1} - h_{r,in})}{q_g \cdot \alpha} \quad (10)$$

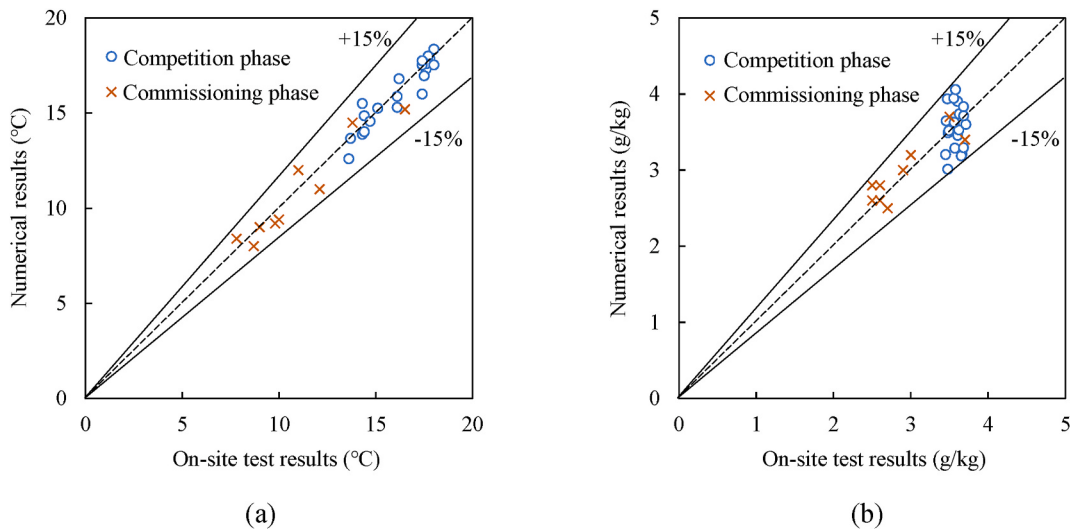


Fig. 2. Model validation: (a) feed air temperature difference between the inlet and outlet of the desiccant wheel (Δt_a), and (b) feed air humidity ratio difference between the inlet and outlet of the desiccant wheel ($\Delta \omega_a$).

where V_g is the nature gas consumption in volume, $Q_{h,I}$ is the heating capacity provided by Heater I, $h_{r,1}$ and $h_{r,in}$ are specific enthalpy values of generation air at R_1 and R_{in} , respectively, q_g is the lower calorific value of nature gas, and α is the convention factor, with a value of 0.2 $m^3\text{-gas}/kWh\text{-electricity}$ according to the national standard [29].

2.4.2. Carbon emission intensity

Carbon emission reduction is essential to mitigate global warming, and thus carbon emission intensity of the regeneration process (CEI_{reg}) is introduced as Eq. (11).

$$CEI_{reg} = P_{h,I} \cdot \xi_e + V_g \cdot \xi_g \quad (11)$$

where ξ_e is the carbon emission factor of electricity, with a value of 0.58 $\text{kg-CO}_2/\text{kWh}\text{-electricity}$ [30], and ξ_g is the carbon emission factor of nature gas, with value of 2.00 $\text{kg-CO}_2/m^3\text{-gas}$ [30,31].

3. Results

3.1. System on-site performance

On-site test results during the test event on October 23, 2021 will be presented in this section, and the test data help figure out the air handling requirements and predict the system performance during the 2022 Winter Olympics. The test results at intervals of 1 h are extracted out and listed in Table 3. The ethylene glycol temperatures at the

entrance of the coolers are $-1.0\text{--}1.2^\circ\text{C}$, while the hot water temperature at the entrance of Heater I is $43.3\text{--}45.1^\circ\text{C}$. To validate the accuracy of the test results, energy and mass unbalance rates are introduced as Eqs. (12) and (13), respectively. Seen from Table 3, both of δ_H and δ_m are within 10%. In consequence, the accuracy of the test results is validated.

$$\delta_H = \frac{2|m_a(h_{a,1} - h_{a,2}) - m_r(h_{r,out} - h_{r,2})|}{m_a(h_{a,1} - h_{a,2}) + m_r(h_{r,out} - h_{r,2})} \quad (12)$$

$$\delta_m = \frac{2|m_a(\omega_{a,1} - \omega_{a,2}) - m_r(\omega_{r,out} - \omega_{r,2})|}{m_a(\omega_{a,1} - \omega_{a,2}) + m_r(\omega_{r,out} - \omega_{r,2})} \quad (13)$$

During the test event, two steams of return air from indoors are used as the regeneration air and feed air, respectively. The demand supply air state during the Winter Olympics can be estimated according to Table 3. The demand supply air temperature ranges $2.5\text{--}3.3^\circ\text{C}$, and the demand supply air humidity ratio ranges $0.3\text{--}0.5 \text{ g/kg}$. In addition, air temperature and humidity near the ice surface were monitored during the test event to estimate the return air parameters during the Olympic period. Four probes were laid out at different height levels over the ice surface, as shown in Fig. 3 (c). Air temperature and humidity distributions above the ice are depicted in Fig. 3 (a) and (b), respectively. It has to be noted that the air temperature and humidity ratio in Fig. 3 (a) and (b) are lower than those of return air (A_{in} and R_{in}) in Table 3, because the audience and competition spaces are open to each other, and the air around the ice surface is mixed with the air near the auditorium and then flows into the desiccant wheel system. In consequence, the temperature

Table 3

Test results ($m_a = 3.8 \text{ kg/s}$, $m_r = 1.6 \text{ kg/s}$).

Time	A_{in} (R_{in})		A_1		A_2		A_{out}		R_1		R_2		R_{out}		Unbalance rate		COP_{reg}		CEI_{reg}		
			t	ω	t	ω	t	ω	t	ω	t	ω	t	ω	δ_H	δ_m					(kg/h)
	(°C)	(g/kg)	(°C)	(g/kg)	(°C)	(g/kg)	(°C)	(g/kg)	(°C)	(g/kg)	(°C)	(g/kg)	(°C)	(g/kg)	(%)	(%)					
8:00	13.1	4.3	3.4	4.3	16.4	0.4	2.5	0.4	39.7	70.1	39.8	13.3	4.1	2.9	0.53	36.7					
9:00	13.5	4.5	3.7	4.5	16.7	0.4	2.7	0.4	40.2	71.5	41.1	13.9	8.0	2.5	0.54	37.6					
10:00	13.9	4.6	3.6	4.6	16.5	0.3	2.6	0.3	40.0	71.5	41.2	14.9	8.1	1.3	0.57	37.5					
11:00	14.2	4.5	4.0	4.5	17.1	0.5	3.2	0.5	40.1	72.5	41.8	13.8	8.3	2.1	0.52	38.3					
12:00	14.9	4.4	4.1	4.4	17.0	0.4	3.2	0.4	40.2	72.8	42.1	13.9	4.7	2.2	0.53	38.3					
13:00	15.5	4.2	4.1	4.2	17.2	0.3	3.0	0.3	40.3	73.3	42.5	13.5	0.6	0.4	0.51	38.5					
14:00	16.1	4.1	4.4	4.1	16.9	0.3	3.1	0.3	40.5	73.0	43.1	13.5	9.1	4.2	0.50	37.9					
15:00	16.3	4.2	4.6	4.2	16.8	0.3	3.3	0.3	40.4	73.0	43.8	13	5.6	5.1	0.52	37.9					
16:00	16.3	4.3	4.3	4.3	16.0	0.3	3.0	0.3	40.3	72.5	43.6	13.7	4.7	0.8	0.53	37.5					
17:00	16.2	4.3	4.4	4.3	16.1	0.4	3.2	0.4	40.4	71.8	44.2	13.3	5.1	3.2	0.53	36.9					
18:00	15.9	4.2	4.2	4.2	16.3	0.3	3.1	0.3	40.3	73.0	43.3	13.2	5.4	2.9	0.51	38.1					

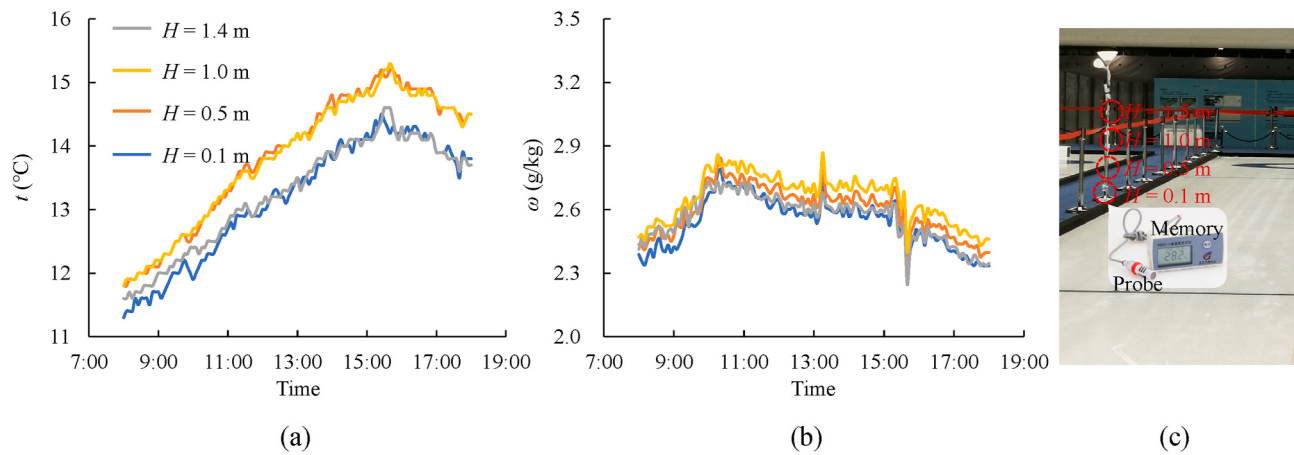


Fig. 3. Air parameter above the ice: (a) air temperature, (b) air humidity ratio, and (c) measuring point positions.

of air from indoors ranges $13.1\text{--}16.3$ °C, and the humidity of air from indoors ranges $4.1\text{--}4.6$ g/kg. In summary, return air and demand supply air parameters during the Winter Olympics can be estimated according to the on-site test results.

3.2. Performance prediction for Winter Olympics

As both outdoor air and indoor air can be used as the regeneration air when achieving the same air dehumidification process, which selection can lead to better energy performance will be elaborated in this section. The Winter Olympics will be hosted in February of 2022. Compared to indoor air temperature and humidity (A_{in} in Table 3), outdoor air is low-temperature and low-humidity in February in Beijing. Thus, the outdoor air is assigned to be used as the feed air. Regeneration energy consumption difference between the following two strategies will be investigated for providing regeneration air selection recommendation:

- Strategy I: Using outdoor air as the regeneration air
- Strategy II: Using indoor air as the regeneration air

3.2.1. Basic case

Outdoor air parameters in Beijing in February of 2022 are estimated based on the weather data in 2021, as shown in Fig. 4 (a). According to the upper and lower quartiles, outdoor air temperature and humidity ratio mainly range $-1.2\text{--}6.9$ °C and $1.1\text{--}2.6$ g/kg in February, respectively. Outdoor air parameters in the basic case are assigned according

to the medians of the values. Similarly, the return air and supply air parameters in the basic case are assigned according to the medians of the tested values at A_{in} and A_{out} , as shown in Fig. 4 (b) and (c). In consequence, the assigned air parameters in the basic case are as listed in Table 4.

The supply air humidity is regulated by the input power of Heater II. When using the mathematical model of the desiccant wheel, each input power corresponds to a certain regeneration temperature ($t_{r,2}$) leading to a certain supply air humidity. The required input power of Heater II and the required regeneration temperature for achieving the demand supply air humidity can be determined by the iteration procedure. Simulation results under the basic case in the two strategies are listed in Table 5, and the corresponding air parameters during the handling processes are depicted in Fig. 5. According to the on-site test results in Section 3.1, the heat exchanger effectiveness of Heater I is 0.84, and then the air temperature at the exit of Heater I can be estimated according to Eq. (8) when assuming the hot water in Heater I at an inlet temperature of 45 °C. Seen from Table 5, Strategy I leads to a lower regeneration

Table 4

Air parameters in the basic case ($m_a = 3.8$ kg/s, $m_r = 1.6$ kg/s).

Demand supply air (A_{out})		Indoor air (return air) (R_{in})		Outdoor air (A_{in} , R_{in})	
t (°C)	ω (g/kg)	t (°C)	ω (g/kg)	t (°C)	ω (g/kg)
3.2	0.4	15.0	4.4	3.5	1.9

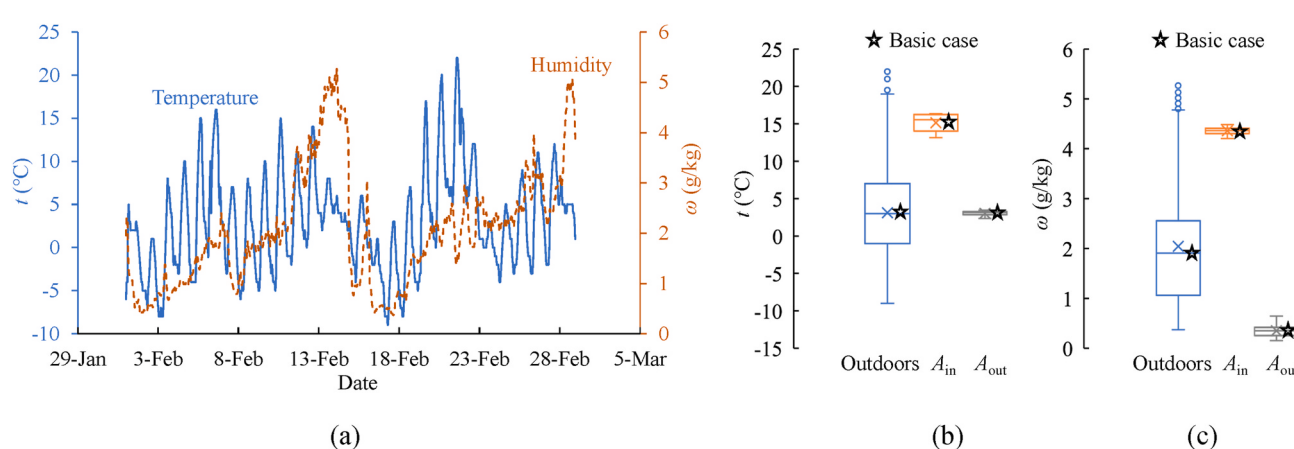


Fig. 4. Air parameters: (a) Outdoor air temperature and humidity in Beijing in February 2021, (b) outdoor air and feed air temperature, and (c) outdoor air and feed air humidity.

Table 5Simulation results in the basic case ($m_a = 3.8 \text{ kg/s}$, $m_r = 1.6 \text{ kg/s}$).

		Strategy I	Strategy II
Feed air	A_{in}	3.5 °C, 1.9 g/kg	3.5 °C, 1.9 g/kg
	A_1	3.5 °C, 1.9 g/kg	3.5 °C, 1.9 g/kg
	A_2	8.9 °C, 0.4 g/kg	9.2 °C, 0.4 g/kg
	A_{out}	3.2 °C, 0.4 g/kg	3.2 °C, 0.4 g/kg
Regeneration air	R_{in}	3.5 °C, 1.9 g/kg	15.0 °C, 4.4 g/kg
	R_1	38.4 °C, 1.9 g/kg	40.2 °C, 4.4 g/kg
	R_2	39.0 °C, 1.9 g/kg	53.5 °C, 4.4 g/kg
	R_{out}	26.2 °C, 5.4 g/kg	40.0 °C, 7.9 g/kg
Performance	$\Delta\omega (\text{g/kg})$	1.5	1.5
	COP_{reg}	0.48	0.34
	$\text{CEI}_{reg} (\text{kg/h})$	12.0	20.7

temperature of 39.0 °C than strategy II (53.5 °C). Consequently, Strategy I results in a better COP_{reg} and a lower CEI_{reg} in comparison to Strategy II, as shown in Fig. 6. COP_{reg} in Strategy I is 41.2% greater than that in Strategy II, and the carbon emission of the regeneration process can be reduced by 42.0% by Strategy I in the basic case.

The reason for the performance difference between the two strategies will be elaborated as follows. On the one hand, the mass transfer driving force during the desiccant regeneration process is the vapor pressure difference between the air and desiccant. When using the air with a higher humidity ratio (vapor pressure) as the regeneration air, the desiccant has to be heated to a higher temperature to maintain the mass transfer driving force. Thus, using the high-humidity indoor air as the regeneration air leading to a higher required regeneration temperature. The regeneration temperature reduction by using a low-humidity air is abbreviated as Δt_1 . On the other hand, a lower inlet air temperature is not conducive to regeneration energy saving, because heating the

lower-temperature air to the same required regeneration temperature indicates more energy consumption. The temperature difference between the indoor air and outdoor air is abbreviated as Δt_2 . Using which air as the regeneration air can bring about energy advantage depends on the relative size of Δt_1 and Δt_2 . If Δt_1 is significantly greater than Δt_2 , Strategy I is recommended. Otherwise, Strategy II is recommended. As listed in Table 5, $\Delta t_1 = 14.5$ °C and $\Delta t_2 = 11.5$ °C. Because $\Delta t_1 > \Delta t_2$ under the basic case, Strategy I is recommended. In addition, two different heaters are installed in the objective system as the heat source, and Heater I is a hot water to air heat exchanger while Heater II is an electric heater. Owing to the difference of the energy grade, the equivalent electricity consumption of Heater I ($P_{h,I}$) is lower than that of Heater II ($P_{h,II}$) when providing the same heating capacity. Using the low-grade energy source (Heater I) as the pre-heater further enhances the energy saving effect of the regeneration temperature reduction by using a low-humidity air steam for regeneration, because the regeneration temperature reduction corresponds to the $P_{h,II}$ saving while using high-temperature air as the regeneration air corresponds to the $P_{h,I}$ saving.

Moreover, Table 6 compares performance of the objective system to performances of other systems from the literature. In general, Q_{latent}/Q_{reg} values in the lower half of Table 6 are greater than the values in the upper half, indicating that, compared to using high-humidity outdoor air as the regeneration air, using low-humidity indoor air contributes to saving regeneration energy consumption when achieving a similar supply air humidity ratio.

3.2.2. Regeneration air recommendation

System performances in Strategy I and Strategy II in February in Beijing will be investigated and compared with each other in this

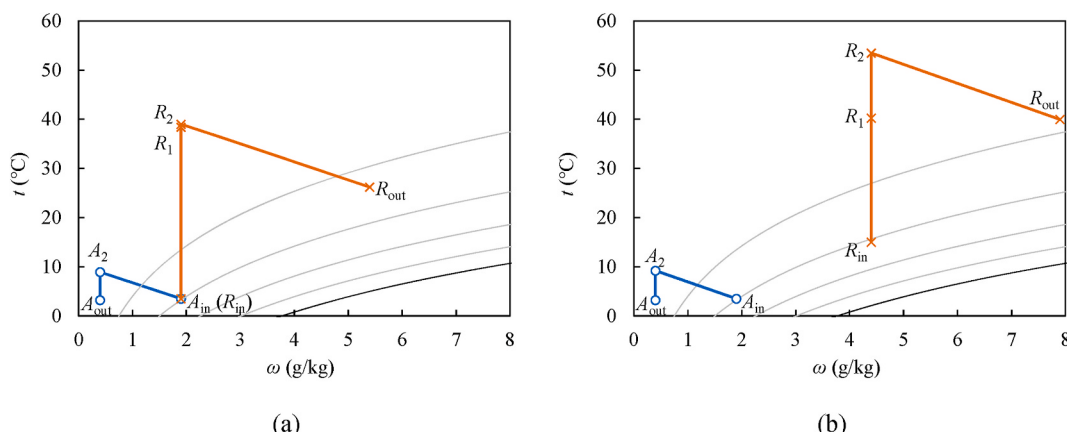


Fig. 5. Air handling process: (a) when using outdoor air as the regeneration air (Strategy I), and (b) when using indoor air as the regeneration air (Strategy II).

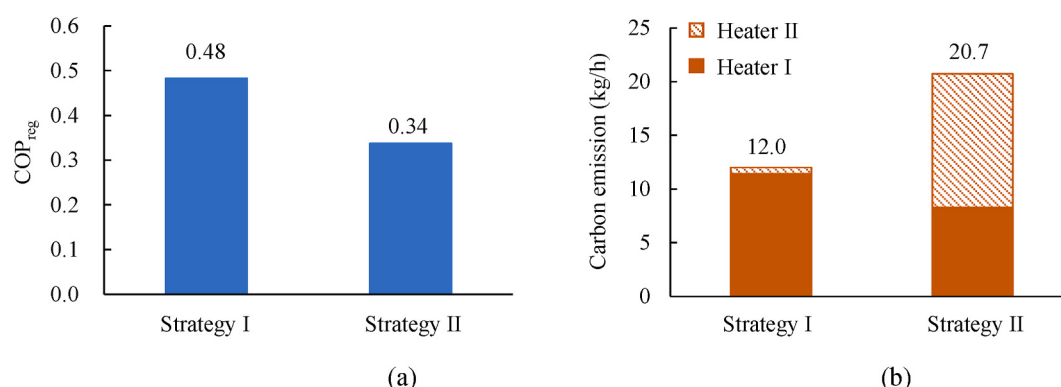


Fig. 6. Performance comparison between Strategies I and II in basic case: (a) COP_{reg} and (b) carbon emission intensity for regeneration (CEI_{reg}).

Table 6

Performance results of the desiccant wheel systems in the literature.

	Regeneration air	Desiccant material	t_{reg} (°C)	$\omega_{a,en}$ (g/kg)	$\omega_{a,out}$ (g/kg)	$\omega_{r,en}$ (g/kg)	Q_{latent}/Q_{reg}
Basic case in this study	Outdoor air	Silica gel	39.0	1.9	0.4	1.9	0.25
Angrisani et al. [4]		Silica gel	55.4	12.8	8.8	12.8	0.44
Caliskan et al. [11]		–	60	12.0	8.0	14.1	0.31
Dadi and Jain [19]		Silica gel	60	9.1–11.8	6.2–8.4	–	0.30–0.38
			70	8.4–11.1	5.1–7.8	–	0.22–0.29
			80	7.3–10.9	4.7–7.9	–	0.15–0.19
Tian et al. [26]	Indoor air	Silica gel	40.3–53.2	12.3–13.6	10.4–10.8	12.7–13.1	0.30–0.34
Basic case in this study		Silica gel	53.5	1.9	0.4	4.4	0.23
Saputra et al. [23]		Silica gel	46.4–75.0	15.0	8.2–11.0	10.5	0.35–0.49
Fong and Lee [21]		Silica gel	50	19.0/19.1	12.3–14.6	10.2/11.6	0.44–0.71
			70	19.0/19.2	10.9–13.5	10.2/11.6	0.32–0.5
			90	19.0/19.3	8.6–12.3	10.2/11.6	0.27–0.44

(t_{reg} : regeneration temperature; $\omega_{a,en}$: feed air humidity ratio at the entrance of the desiccant wheel; $\omega_{a,out}$: supply air humidity ratio; $\omega_{r,en}$: regeneration air humidity ratio at the entrance of the desiccant wheel; Q_{reg} : heating capacity consumption for heating regeneration air to the required regeneration temperature).

section. It is assumed that the system operates from 8:00 to 18:00 in February, and the heating consumption as well as the carbon emission during the entire month are simulated.

With reference to the heating consumption for regeneration, the system in Strategy I consumes a total value of 13.9×10^3 kWh. Heater I accounts for 79.3% and Heater II (electric heater) accounts for the remaining 20.7%, as shown in Fig. 7(a). The system in Strategy II consumes a total value of 12.6×10^3 kWh. Heater I accounts for 51.4% and Heater II (electric heater) accounts for the remaining 48.6%. Although the heating consumption difference between the two strategies is less than 10%, the carbon mission in Strategy I is 19.4% lower than that in Strategy II, as shown in Fig. 7(b). Because the required regeneration temperature is reduced by using low-humidity air as the regeneration air in Strategy I, the electric heater (Heater II) is responsible for a

significantly lower proportion of total heating consumption in Strategy I. Moreover, the high-grade heat source (Heater II) corresponds to a higher carbon emission factor than the low-grade heat source (Heater I), and accordingly, Strategy I results in a lower carbon emission, compared to Strategy II.

In summary, outdoor air is recommended as the regeneration air during the 2022 Beijing Winter Olympics, and the carbon emission for the regeneration process can be reduced by 19.4% by using outdoor air as the regeneration air. Moreover, it has to be noted that using a low-grade heat source as a pre-heater can not only improve the system energy performance, but also help reduce system carbon emission.

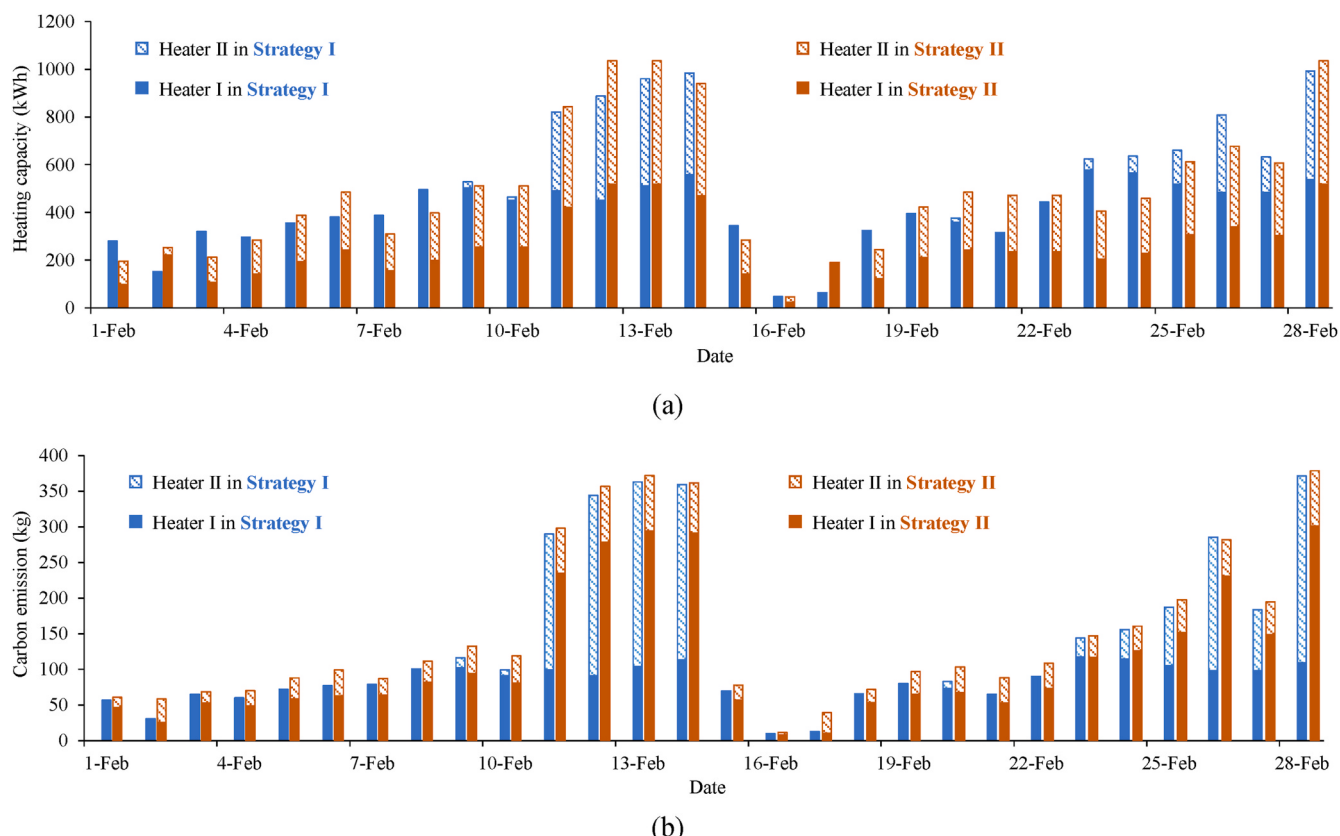


Fig. 7. Performance comparison between Strategies I and II in February: (a) heating consumption, and (b) carbon emission.

4. Discussion

Although the above content provides recommendation for regeneration air selection during the Winter Olympics, there are still two obvious drawbacks: (i) no recommendations have been provided for other scenes; (ii) the complexity and iterative processes of the mathematical model limit its real engineering application. To overcome the drawbacks, a quick and approximate method (simplified method) without iterative processes will be proposed for regeneration air selection in similar scenes.

4.1. Simplified method for regeneration air selection

4.1.1. Ideal outlet air state

The ideal outlet states of the feed air (A_{ideal}) and regeneration air (R_{ideal}) under ideal conditions are presented in Fig. 8. In the psychrometric chart, the ideal outlet state of the feed air (A_{ideal}) is located at the intersection point of the isenthalpic line of A_{in} and the iso-RH line of R_{in} , while the ideal outlet state of the regeneration air (R_{ideal}) is located at the intersection point of the isenthalpic line of R_{in} and the iso-RH line of A_{in} . The iso-RH lines of A_{in} and R_{in} and the isenthalpic lines of A_{in} and R_{in} form the four boundary lines in Fig. 8. The outlet air states of the feed air (A_{out}) and regeneration air (R_{out}) must exist inside the region $A_{\text{in}}A_{\text{ideal}}R_{\text{in}}R_{\text{ideal}}$. There are two prerequisites for achieving A_{ideal} [32,33]: (i) the heat capacities of the wheel substrate and the absorbed moisture are null; (ii) the regeneration air is sufficiently supplied. When Prerequisite (i) valid, the dehumidification process will be an adiabatic process and the enthalpy of A_{out} will be equal to A_{in} . When Prerequisite (ii) valid, the relative humidity of A_{out} will be approximately equal to that of R_{in} [34,35]. Similarly, there are also two ideal assumptions for achieving R_{ideal} [32,33]: (i) the heat capacities of the wheel substrate and the absorbed moisture are null; (ii) the regeneration air is insufficiently supplied. When Prerequisite (i) valid, the regeneration process will be an adiabatic process and the enthalpy of R_{out} will be equal to R_{in} . When Prerequisite (ii) valid, the relative humidity of A_{out} will be approximately equal to that of A_{in} [34,35].

It is important for the supply air A_{out} to approach its minimum (A_{ideal}), for exerting the dehumidification ability of the desiccant. An optimal rotation speed (RS) is necessary for A_{out} to approach its minimum. The effect of RS on the objective desiccant wheel in Section 3.2 is shown in Fig. 9 (a). The outlet air condition changes along the arrow line, and $A_{\text{out}}/R_{\text{out}}$ approaches its minimum/maximum when RS ≈ 10 r/h, indicating an optimal RS around 10 r/h. Further increase of the RS induces deviation of A_{out} from the ideal isenthalpic line $A_{\text{in}}A_{\text{ideal}}$. This is because of the infinite heat capacities of the substance and absorbed moisture, and correspondingly, the sensible heat transfer between the dehumidification and regeneration sections through the wheel increases with the RS increasing. Moreover, effect of the regeneration air flow rate

(m_r/m_a) on the outlet air state is shown in Fig. 9(b). When m_r/m_a above 0.3, the regeneration air is sufficient and RH of A_{out} is approximately equal to RH of R_{in} . While when m_r/m_a below 0.2, the regeneration air is insufficient and RH of A_{out} is approximately equal to RH of A_{in} .

In summary, the closet approach of A_{out} to its minimum (A_{ideal}) occurs when the regeneration air is sufficient and the wheel operates at its optimal RS.

4.1.2. Method development

In engineering applications, the optimal RS and sufficient regeneration air supply can be achieved by pre-commissioning. Under the above pre-conditions, the flowchart for the regeneration air selection without iterative algorithm is shown in Fig. 10. The configuration of the typical desiccant wheel system is shown in Fig. 10 (a). The core of the method is to determine the required regeneration temperature (air temperature at R_{reg}) according to states of A_{in} and R_{in} and the demand state of A_{out} . As the isenthalpic process assumption, $h_{\text{a,out}} \approx h_{\text{a,in}}$, and thus, RH_{a,out} can be calculated based on the demand $\omega_{\text{a,out}}$ and the obtained $h_{\text{a,out}}$. When the regeneration air is sufficient, RH_{a,out} \approx RH_{r,reg}, and RH_{r,reg} can be obtained. Accordingly, the required regeneration temperature $t_{r,reg}$ can be obtained according the known $\omega_{\text{r,in}}$ ($\omega_{\text{r,reg}}$) and RH_{r,reg}. Then, the regeneration temperature difference between the two strategies (Δt_1) can be calculated, as well as the inlet air temperature difference between the two strategies (Δt_2). Which strategy is recommended depends on the relative size of Δt_1 and Δt_2 .

4.2. Applicability analysis

The accuracy and applicability of the proposed simplified model will be discussed in this section. The key step of the model is to predict the regeneration temperature, and accordingly, the accuracy of the model relies on the accuracy of the regeneration temperature prediction.

Taking the objective system on February 15, 2022 for example, results by the mathematical model (Section 2.3) and the simplified model (Section 4.1) are listed in Table 7. The required regeneration temperatures by the mathematical model and by the simplified model are respectively 15.2–34.3 °C and 12.0–30.6 °C in Strategy I, while they are respectively 39.1–53.3 °C and 36.0–50.2 °C in Strategy II. The regeneration temperature prediction deviation between the mathematical model and the simplified model ranges 0.3–4.5 °C. The regeneration temperature is underestimated by the simplified model compared with the mathematical model, due to the isenthalpic dehumidification/regeneration process assumption. Moreover, the regeneration temperature difference between the two strategies (Δt_1) is depicted in Fig. 11. As presented in Fig. 11, Δt_1 by the mathematical model is similar to that by the simplified model, and the deviation is below 3 °C, indicating the method can be adopted to provide regeneration air selection recommendation. In addition, the deviation of Δt_1 is lower than that of the regeneration temperature. This is because both the regeneration temperatures under Strategy I and Strategy II are underestimated by the simplified model. Accordingly, the underestimations are offset with each other, to a certain extent, when calculating Δt_1 .

To further discuss the applicable scene of the simplified model, the effect of the moisture removal amount on the deviation between the mathematic model and the simplified method is shown in Fig. 12. As depicted in Fig. 12 (a), the underestimation effect of the simplified model increases with the increase of the dehumidification depth, due to the isenthalpic dehumidification process assumption. When the moisture removal amount of per kilogram air ($\omega_{\text{a,in}} - \omega_{\text{a,out}}$) rises from 2.0 to 5.5 g/kg, the deviation between the outlet air states by the mathematical model and by the simplified model ($A_{\text{out, math}}$ and $A_{\text{out,sim}}$) increases from 1.8 to 6.1 °C. Then the deviation is further amplified by the iso-RH line of A_{out} , and thus, the deviation of the regeneration temperature prediction between the two methods correspondingly rises from 1.9 to 7.0 °C, as shown in Fig. 12 (a). Regarding the included angle between lines of $A_{\text{in}}A_{\text{out, math}}$ and $A_{\text{in}}A_{\text{out,sim}}$ (isenthalpic line) as an

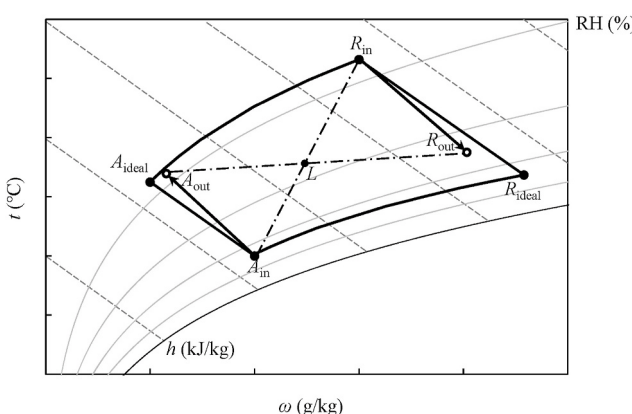


Fig. 8. An example of changes of air states around the desiccant wheel.

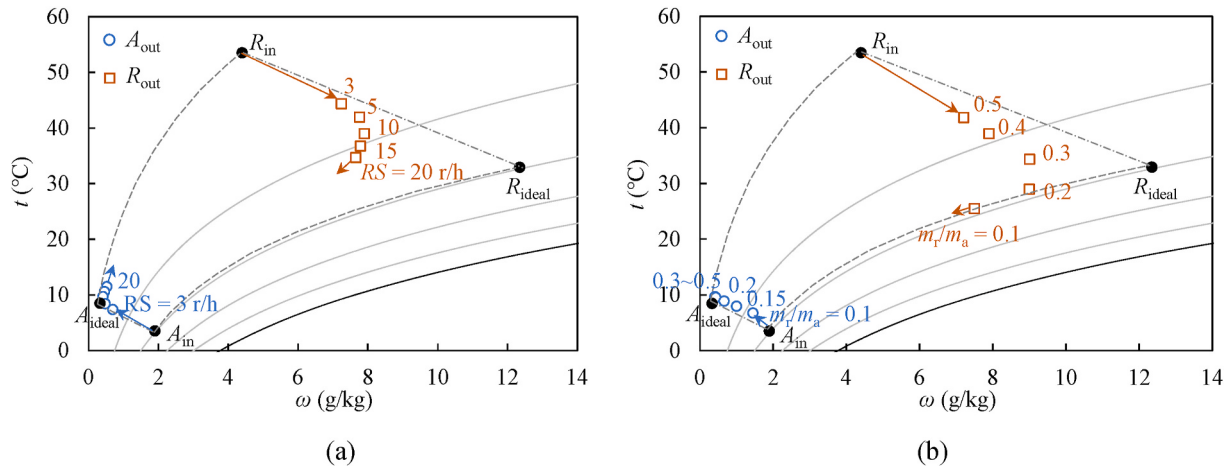


Fig. 9. Variation of feed air and regeneration air states at the exits of the desiccant wheel: (a) when different wheel rotation speeds (RS) increasing, and (b) under different flow rate ratios of regeneration air to feed air (m_r/m_a) decreasing.

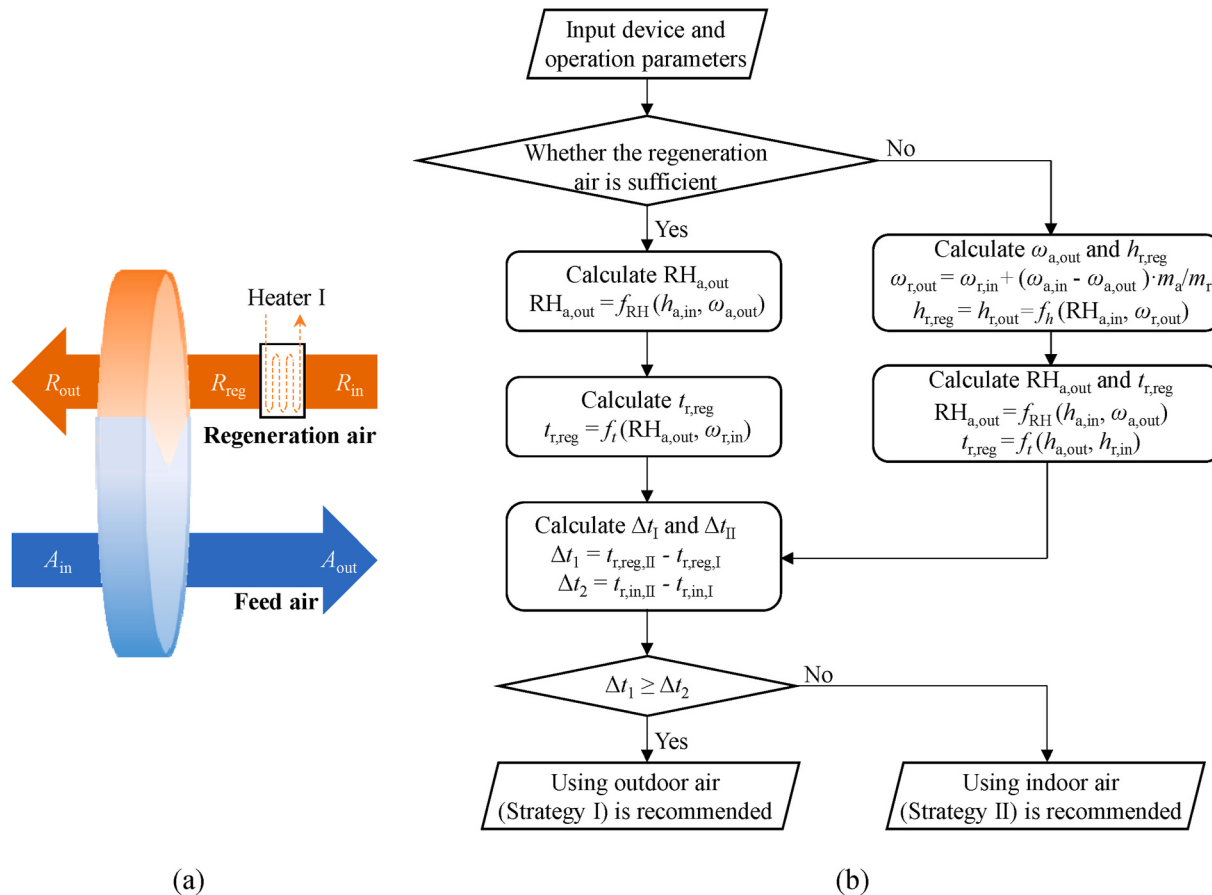


Fig. 10. Flowchart for determining using outdoor or indoor air as the regeneration air: (a) typical configuration of the desiccant wheel system, and (b) flowchart for strategy recommendation.

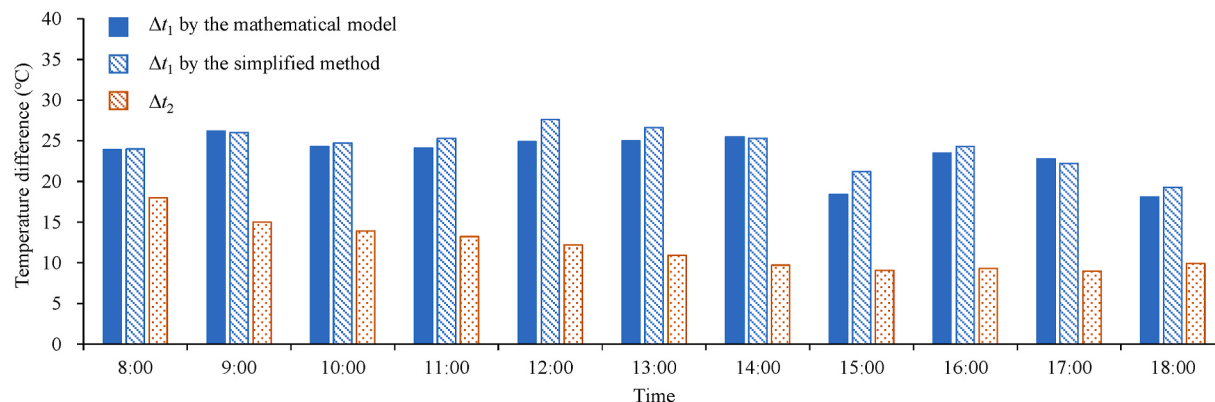
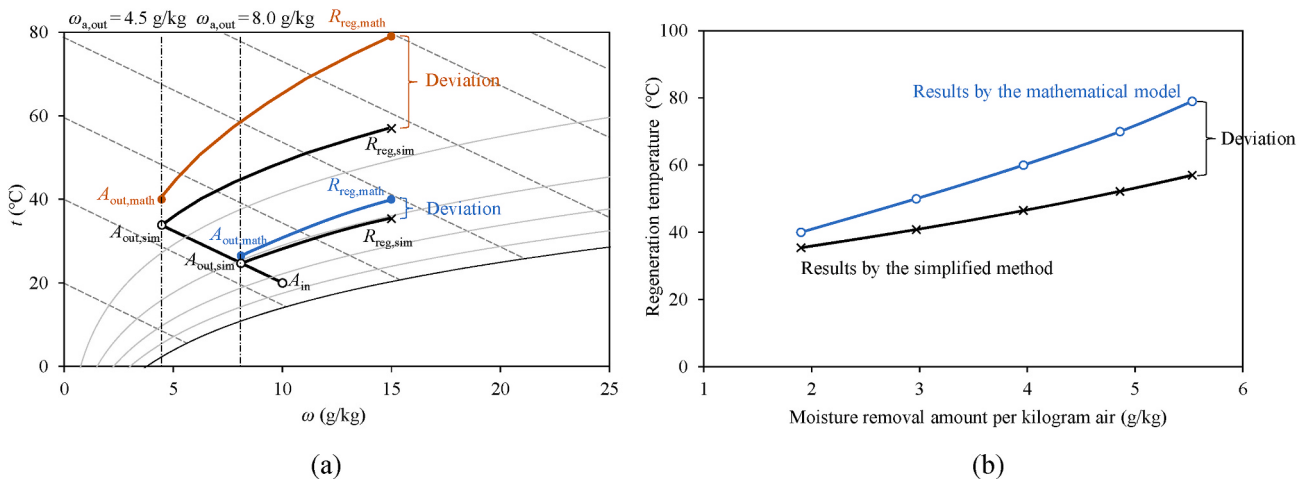
approximately fixed value, the distance between $A_{out, math}$ and $A_{out,sim}$ in the psychrometric chart increases with the increase of $(\omega_{a,in} - \omega_{a,out})$. Consequently, it is indicated that the simplified method applies to environments requiring a low $(\omega_{a,in} - \omega_{a,out})$. As depicted in Fig. 12 (b), the deviation of the regeneration temperature between the two methods is lower than 5 °C when the moisture removal amount $(\omega_{a,in} - \omega_{a,out})$ below 3 g/kg.

The simplified method contributes to determining using indoor or outdoor air as the regeneration air in engineering applications. The

method accuracy improves with the moisture removal amount $(\omega_{a,in} - \omega_{a,out})$ decreasing, indicating the method applies to environments requiring a low $(\omega_{a,in} - \omega_{a,out})$, particularly for those requiring a $(\omega_{a,in} - \omega_{a,out}) < 3$ g/kg, such as the curling arena. There are two main limitations of the model. First, the deviation of the model increases with the moisture removal amount, and thus, the model cannot be used to assess the conventional desiccant wheel dehumidification process, like the office building requiring dehumidifying air humidity from over 20 g/kg to about 10 g/kg in summer. Second, the condensing phenomenon is

Table 7Comparison of results by the mathematical model and the simplified method ($m_a = 3.8 \text{ kg/s}$, $m_r = 1.6 \text{ kg/s}$).

Time	Indoor air		Outdoor air		Supply air	Regeneration temperature		Simplified method	
						Mathematical model		Simplified method	
	t (°C)	ω (g/kg)	t (°C)	ω (g/kg)	ω (g/kg)	Strategy I (°C)	Strategy II (°C)	Strategy I (°C)	Strategy II (°C)
8:00	15.0	4.4	-3.0	0.9	0.4	15.2	39.1	12.0	36.0
9:00			0.0	0.9		17.0	43.2	14.5	40.5
10:00			1.1	1.0		20.5	44.8	17.3	42.0
11:00			1.8	1.0		21.9	46.0	17.5	42.8
12:00			2.8	1.0		22.8	47.7	18.3	45.7
13:00			4.1	0.9		23.5	48.5	19.4	46.0
14:00			5.3	1.1		26.2	51.7	22.9	48.2
15:00			5.9	1.1		27.6	46.0	24.5	45.7
16:00			5.7	1.1		28.1	51.6	24.7	49.0
17:00			6.0	1.3		30.5	53.3	28.0	50.2
18:00			5.1	1.6		34.3	52.4	30.6	49.9

**Fig. 11.** Regeneration air recommendations by the mathematic model and the simplified method.**Fig. 12.** Effect of the moisture removal amount on the deviation between the mathematic model and the simplified method: (a) deviation shown in the psychrometric chart, and (b) deviation of the regeneration air temperature.

ignored in the model. The absorbent temperature is below 0 °C on the dehumidification side. When the regeneration air has a high humidity ratio, the moisture in the regeneration air may be condensed onto the surface of the part of the absorbent just rotating to the regeneration side. This phenomenon can occur when the wheel rotation speed is high. However, in ice arenas, the rotation speed is usually below 30 r/h to dehumidify the supply air to a low humidity ratio. The low rotation speed makes the absorbent just rotating to the regeneration side

sufficiently heated by the high-temperature regeneration air, and thus, the phenomenon is rarely observed and can be ignored in this circumstance.

5. Conclusions

For achieving energy conservation and carbon emission reduction, regeneration energy performance of the desiccant system in the

Winter Olympic curling arena is investigated in this study. Both the outdoor air and indoor air can be used as the regeneration air when accomplishing the same air dehumidification process, and the regeneration air selection recommendation is provided based on the on-site test and simulation results. Moreover, a quick and approximate method for regeneration air selection is developed to provide reference for similar ice rink arenas. Main conclusions are as follows:

- 1) Using outdoor air as the regeneration air is recommended for the desiccant wheel system applied in the curling arena during the 2022 Winter Olympics. In the basic case, the coefficient of regeneration performance can be improved by 41.2% and the carbon emission for the regeneration process can be reduced by 42.0% by using outdoor air for regeneration, compared to using indoor air for regeneration. During the entire February, Beijing Winter Olympic month, the carbon emission during the regeneration process can be reduced by 19.4% by using the outdoor air for regeneration.
- 2) A quick and approximate method without iterative processes is developed for regeneration air selection. The required regeneration temperature is underestimated by the method due to the ideal isenthalpic dehumidification/regeneration process assumption. The accuracy of the method is significantly affected by the moisture removal amount ($\omega_{a,in} - \omega_{a,out}$) demand, indicating the method applies to environments requiring a low moisture removal amount, particularly for those requiring ($\omega_{a,in} - \omega_{a,out}$) below 3 g/kg.

CRediT authorship contribution statement

Bowen Guan: Investigation, Data curation, Writing – original draft, Methodology. **Xiaohua Liu:** Writing – review & editing, Funding acquisition. **Xinke Wang:** Writing – review & editing. **Tao Zhang:** Supervision, Writing – review & editing. **Ziqi Zhou:** Funding acquisition, Writing – review & editing.

Declaration of competing interest

The authors declare that they have no known competing financial interests or personal relationships that could have appeared to influence the work reported in this paper.

Acknowledgments

This research was supported by the National Key Research Program of China (No. 2020YFF0304303, 2020YFF0304302), the Development Program of CSCEC (CSCEC-2019-Z-7) and Sichuan Science and Technology Planning Project (2019YFSY0009).

References

- [1] S. Ahmed, Pa Nelson, D.W. Dees, Study of a dry room in a battery manufacturing plant using a process model, *J. Power Sources* 326 (2016) 490–497, <https://doi.org/10.1016/j.jpowsour.2016.06.107>.
- [2] Q. Chen, J.R. Jones, R.H. Archer, A dehumidification process with cascading desiccant wheels to produce air with dew point below 0 degrees C, *Appl. Therm. Eng.* 148 (2019) 78–86, <https://doi.org/10.1016/j.applthermaleng.2018.10.114>.
- [3] B.W. Guan, T. Zhang, X.H. Liu, On-site performance investigation of a desiccant wheel deep-dehumidification system applied in lithium battery manufacturing plant, *Energy Build.* 232 (2021) 110659, <https://doi.org/10.1016/j.enbuild.2020.110659>.
- [4] G. Angrisani, F. Minichiello, C. Roselli, et al., Experimental analysis on the dehumidification and thermal performance of a desiccant wheel, *Appl. Energy* 92 (2012) 563–572, <https://doi.org/10.1016/j.apenergy.2011.11.071>.
- [5] M.K. Shahzad, G.Q. Chaudhary, M. Ali, et al., Experimental evaluation of a solid desiccant system integrated with cross flow Maisotsenko cycle evaporative cooler, *Appl. Therm. Eng.* 128 (2018) 1476–1487, <https://doi.org/10.1016/j.applthermaleng.2017.09.105>.
- [6] Rang Tu, J.Q. Li, T. Hwang, Performance analysis of desiccant wheels assisted fresh air humidifiers in winter using natural gas boilers: applied in cold and dry climate regions, *Int. J. Refrig.* 119 (2020) 24–36, <https://doi.org/10.1016/j.ijrefrig.2020.08.003>.
- [7] H. Kang, D.Y. Lee, Experimental investigation and introduction of a similarity parameter for characterizing the heat and mass transfer in polymer desiccant wheels, *Energy* 120 (2017) 705–717, <https://doi.org/10.1016/j.energy.2016.11.122>.
- [8] C. Aprea, A. Greco, A. Maiorino, The application of a desiccant wheel to increase the energetic performances of a transcritical cycle, *Energy Convers. Manag.* 89 (2015) 222–230, <https://doi.org/10.1016/j.enconman.2014.09.066>.
- [9] H. Kamar, N. Kamsah, M.I. Alhamid, et al., Effect of regeneration air temperature on desiccant wheel performance, *International Journal of Technology* 7 (2016) 281–287, <https://doi.org/10.14716/ijtech.v7i2.2971>.
- [10] G. Angrisani, A. Capozzoli, F. Minichiello, et al., Desiccant wheel regenerated by thermal energy from a microcogenerator: experimental assessment of the performances, *Appl. Energy* 88 (2011) 1354–1365, <https://doi.org/10.1016/j.apenergy.2010.09.025>.
- [11] H. Caliskan, D.Y. Lee, H. Hong, Enhanced thermodynamic assessments of the novel desiccant air cooling system for sustainable energy future, *J. Clean. Prod.* 211 (2019) 213–221, <https://doi.org/10.1016/j.jclepro.2018.11.174>.
- [12] A. Rjibi, S. Kooli, A. Guizani, The effects of regeneration temperature of the desiccant wheel on the performance of desiccant cooling cycles for greenhouse thermally insulated, *Heat Mass Tran.* 54 (2018) 3427–3443, <https://doi.org/10.1007/s00231-018-2369-4>.
- [13] H.S. Ren, Z.H. Ma, W.Y. Lin, et al., Integrating photovoltaic thermal collectors and thermal energy storage systems using phase change materials with rotary desiccant cooling systems, *Sustain. Cities Soc.* 36 (2018) 131–143, <https://doi.org/10.1016/j.scs.2017.10.021>.
- [14] Y.F. Liu, Y.Y. Chen, D.J. Wang, et al., Performance evaluation of a hybrid solar powered rotary desiccant wheel air conditioning system for low latitude isolated islands, *Energy Build.* 224 (2020) 110208, <https://doi.org/10.1016/j.enbuild.2020.110208>.
- [15] L. Chen, W.J. Deng, Y.J. Chu, Experimental study on desiccant evaporative combined chilled air/chilled water air conditioning systems, *Appl. Therm. Eng.* 199 (2021) 117534, <https://doi.org/10.1016/j.applthermaleng.2021.117534>.
- [16] M. El Loubani, N. Ghaddar, K. Ghali, M. Itani, Hybrid cooling system integrating PCM-desiccant dehumidification and personal evaporative cooling for hot and humid climates, *J. Build. Eng.* 33 (2021) 101580, <https://doi.org/10.1016/j.jobe.2020.101580>.
- [17] X.C. Zhou, Thermal and energy performance of a solar-driven desiccant cooling system using an internally cooled desiccant wheel in various climate conditions, *Appl. Therm. Eng.* 185 (2021) 116077, <https://doi.org/10.1016/j.applthermaleng.2020.116077>.
- [18] F. Comino, F. Tobaso, F. Peci, et al., Detailed experimental analysis of the energy performance of a desiccant wheel activated at low temperature, *Appl. Therm. Eng.* 178 (2020) 115580, <https://doi.org/10.1016/j.applthermaleng.2020.115580>.
- [19] M.J. Dadi, D.B. Jani, Experimental investigation of solid desiccant wheel in hot and humid weather of India, *Int. J. Ambient Energy* (2021), <https://doi.org/10.1080/01430750.2021.1999326>.
- [20] M. Ukai, H. Tanaka, H. Tanaka, et al., Performance analysis and evaluation of desiccant air-handling unit under various operation condition through measurement and simulation in hot and humid climate, *Energy Build.* 172 (2018) 478–492, <https://doi.org/10.1016/j.enbuild.2018.04.040>.
- [21] K.F. Fong, C.K. Lee, New perspectives in solid desiccant cooling for hot and humid regions, *Energy Build.* 158 (2018) 1152–1160, <https://doi.org/10.1016/j.enbuild.2017.11.016>.
- [22] A.E. Kabeel, M. Abdelgaid, Solar energy assisted desiccant air conditioning system with PCM as a thermal storage medium, *Renew. Energy* 122 (2018) 632–642, <https://doi.org/10.1016/j.renene.2018.02.020>.
- [23] D.A. Saputra, Y. Osaka, T. Tsujiguchi, et al., Experimental investigation of desiccant wheel dehumidification control method for changes in regeneration heat input, *Energy* 205 (2020) 118109, <https://doi.org/10.1016/j.energy.2020.118109>.
- [24] M.F. Habib, M. Ali, N.A. Sheikh, et al., Building thermal load management through integration of solar assisted absorption and desiccant air conditioning systems: a model-based simulation-optimization approach, *J. Build. Eng.* 30 (2020) 110279, <https://doi.org/10.1016/j.jobe.2020.101279>.
- [25] G. Heidarinejad, S. Rayegan, H. Pasdarshahr, Dynamic simulation of a solar desiccant cooling system combined with a ground source heat exchanger in humid climates, *J. Build. Eng.* 28 (2020) 101048, <https://doi.org/10.1016/j.jobe.2019.101048>.
- [26] S.C. Tian, X. Su, H. Li, et al., Using a coupled heat pump desiccant wheel system to improve indoor humidity environment of nZEB in Shanghai: analysis and optimization, *Build. Environ.* 206 (2021) 108391, <https://doi.org/10.1016/j.buildenv.2021.108391>.
- [27] A. Asadi, B. Roshanzadeh, Improving performance of two-stage desiccant cooling system by analyzing different regeneration configurations, *J. Build. Eng.* 25 (2019) 100807, <https://doi.org/10.1016/j.jobe.2019.100807>.
- [28] R. Tu, X.H. Liu, Y. Jiang, Performance comparison between enthalpy recovery wheels and dehumidification wheels, *Int. J. Refrig.* 36 (2013) 2308–2322, <https://doi.org/10.1016/j.ijrefrig.2013.07.014>.
- [29] Standardization Administration, Classification and Presentation of Civil Building Energy Use. GB/T 34913-2017, Standards Press of China, Beijing, 2017.
- [30] Q.Y. Wang, Energy data, cited on 2021-12-18, <https://www.efchina.org/Reports-zh/report-lceg-20210430-3-zh>, 2020.
- [31] Standardization Administration, General Rules for Calculation of the Comprehensive Energy Consumption. GB/T 2589-2020, Standards Press of China, Beijing, 2020.

- [32] A. Kodama, T. Hirayama, M. Goto, et al., The use of psychrometric charts for the optimisation of a thermal swing desiccant wheel, *Appl. Therm. Eng.* 21 (2002) 1657–1674, [https://doi.org/10.1016/S1359-4311\(01\)00032-1](https://doi.org/10.1016/S1359-4311(01)00032-1).
- [33] H. Kang, D.Y. Lee, Experimental investigation and introduction of a similarity parameter for characterizing the heat and mass transfer in polymer desiccant wheels, *Energy* 120 (2017) 705–717, <https://doi.org/10.1016/j.energy.2016.11.122>.
- [34] M.O. Carpinlioglu, M. Yildirim, A methodology for the performance evaluation of an experimental desiccant cooling system, *Int. Commun. Heat Mass Tran.* 32 (2005) 1400–1410, <https://doi.org/10.1016/j.icheatmasstransfer.2005.07.008>.
- [35] C.R. Ruivo, J.J. Costa, A.R. Figueiredo, et al., Effectiveness parameters for the prediction of the global performance of desiccant wheels e an assessment based on experimental data, *Renew. Energy* 38 (2012) 181–187, <https://doi.org/10.1016/j.renene.2011.07.023>.